Measures of resolution in global body wave tomography

L. Boschi
Università di Napoli Federico II, Dipartimento di Fisica, Naples, Italy

Received 22 June 2003; accepted 6 August 2003; published 3 October 2003.

[1] The resolution of tomographic images is most often evaluated through synthetic tests: the inversion algorithm used to derive the image itself is applied to a synthetic data set having the same source-station geometry of the real one, but theoretical travel times computed from a chosen "input model" (e.g., a checkerboard). The similarity between input model and solution of the synthetic test, used as a measure of resolution, has the major shortcoming of depending on the choice of the input model. Conversely, the similarity of the "model resolution matrix" (R) to the identity matrix is a rigorous measure of resolution that does not depend on any input model, but has the drawback of being computationally heavy. In the past decade, several authors have devised complicated algorithms for the approximate or iterative derivation of R. I show here that parallel Cholesky factorization of $\mathsf{A}^T \cdot \mathsf{A}$ (A being the matrix that identifies the linear inverse problem), feasible on shared-memory multiprocessor servers, provides an efficient way of determining both least squares solutions and resolution matrices in global tomography. I apply this procedure in an evaluation of the resolution of mantle structure from a global *P*-wave travel time data set. *INDEX TERMS:* 3260 Mathematical Geophysics: Inverse theory; 7207 Seismology: Core and mantle; 8124 Tectonophysics: Earth's interior—composition and state (1212); 8180 Tectonophysics: Tomography. **Citation:** Boschi, L., Measures of resolution in global body wave tomography, *Geophys. Res. Lett.*, *30*(19), 1978, doi:10.1029/2003GL018222, 2003.

1. Introduction

[2] Tomographic images cannot reproduce the true structure of the Earth's interior at all spatial wavelengths. Current global tomographic models of the Earth are known to be reliable at long wavelengths, where results of different approaches are consistent, but become less so as wavelength decreases [*Boschi and Dziewonski*, 1999; *Becker and Boschi*, 2002].

[3] The resolution of a tomographic image is the highest spatial frequency at which the image is expected to be meaningful; its value is limited by two factors: the quality of the data and the uniformity of their spatial distribution (the "data coverage"), and the approximations involved in the formulation of the inverse problem.

[4] The latter issue can be relevant for seismic measurements made at periods long enough for the ray-theory approximation to break down [e.g., *Spetzler et al.*, 2002]; it can also be relevant at the crustal scale, where velocity heterogeneities are strong enough to alter significantly the geometry of seismic ray paths [e.g., *Zollo et al.*, 2002]. Here I shall only concern myself with teleseismic *P*-wave travel time observations, and the "theoretical" issue becomes secundary.

[5] If the effect of flaws in the theory is negligible, resolution can be evaluated by "synthetic tests" or, preferably [*Leveque et al.*, 1993; *Nolet et al.*, 1999], deriving the "resolution matrix" associated with the inverse problem in question. Unfortunately, computing the resolution matrix is not a trivial task. Iterative least-squares algorithms like LSQR [*Paige and Saunders*, 1982], now widely used in high-resolution global tomography, do not provide it; several authors [*Vasco et al.*, 1993, 1999, 2003; *Zhang and McMehan*, 1995; *Minkoff*, 1996; *Nolet et al.*, 1999, 2001; *Yao et al.*, 1999, 2001] devised algorithms for its iterative, approximate computation.

[6] I show here that the resolution matrix, and the least-squares solution, of a large global tomographic inverse problem can be calculated exactly, implementing a well known algorithm (parallel Cholesky factorization) on multiprocessor, shared-memory computers that are now of widespread use. I show how this approach can be used to assess the resolution of current *P*-velocity images of the Earth's mantle.

2. The Resolution Matrix

[7] The most common way to quantify the resolution of a seismic data set is through a synthetic test: let the equation

$$\mathsf{A} \cdot \mathsf{x} = \mathsf{d} \tag{1}$$

describe the corresponding tomographic inverse problem, with d the data *m*-vector, x the solution *n*-vector, whose entries are the unknown coefficients of *P*-wave velocity in the mantle with respect to some set of *n* basis functions, and A a $m \times n$ matrix that depends on data coverage and on the choice of basis functions [e.g., *Boschi and Dziewonski*, 1999]; synthetic tests consist of (i) computing a theoretical data vector

$$\mathsf{d}' = \mathsf{A} \cdot \mathsf{x}_{\mathrm{in}}, \tag{2}$$

based on the actual data coverage and a known "input model" x_{in}; (ii) replace d with d' in equation (1); (iii) solve the resulting synthetic inverse problem with the same algorithm applied to the real one. The similarity between the least squares solution thus obtained (the "output" model, $\mathsf{x}_{\mathrm{out}}$) and the input model x_{in} can be interpreted as a measure of resolution. This measure is not optimal, since it strongly depends on the choice of the input model, but it is the one most often seen in global seismology literature. A more rigorous quantification of resolution is the "model resolu-

0094-8276/03/2003GL018222$05.00

tion matrix": it can be shown [e.g., *Trefethen and Bau*, 1997] that the least squares solution x_{LS} of (1) equals

$$\mathsf{x}_{LS} = \left(\mathsf{A}^T \cdot \mathsf{A} + \mathsf{D}\right)^{-1} \cdot \mathsf{A}^T \cdot \mathsf{d}, \tag{3}$$

where the matrix D represents the cumulative effect of the regularization constraints that we impose [*Boschi and Dziewonski*, 1999]; then, if d is replaced by d',

$$\mathsf{x}_{\text{out}} = \left(\mathsf{A}^T \cdot \mathsf{A} + \mathsf{D}\right)^{-1} \cdot \mathsf{A}^T \cdot \mathsf{A} \cdot \mathsf{x}_{\text{in}}. \tag{4}$$

The model resolution matrix is precisely

$$\mathsf{R} = \left(\mathsf{A}^T \cdot \mathsf{A} + \mathsf{D}\right)^{-1} \cdot \mathsf{A}^T \cdot \mathsf{A} \tag{5}$$

[e.g., *Menke*, 1989, equation (4.5)]. Resolution can be quantified, independently of x_{in}, plotting the $n \times n$ matrix R and comparing it to the $n \times n$ identitity matrix I. Clearly, $\mathsf{R} = \mathsf{I}$ in the limit case of perfect resolution. Nonzero off-diagonal entries of R identify model coefficients that tend to "trade-off" with each other: in practice, a nonzero entry at row i, column j of R indicates a trade-off between the i-th and j-th model coefficients, whose entity is proportional to the size of R_{ij}.

[8] R can be thought of as the operator that relates x_{out} and x_{in} in a synthetic test with damping D; it should be kept in mind, however, that iterative algorithms do not involve the direct implementation of (3) and (5): authors that follow the iterative approach must estimate R by iterative approximations [*Yao et al.*, 1999], or through alternative approximate expressions [*Nolet et al.*, 1999].

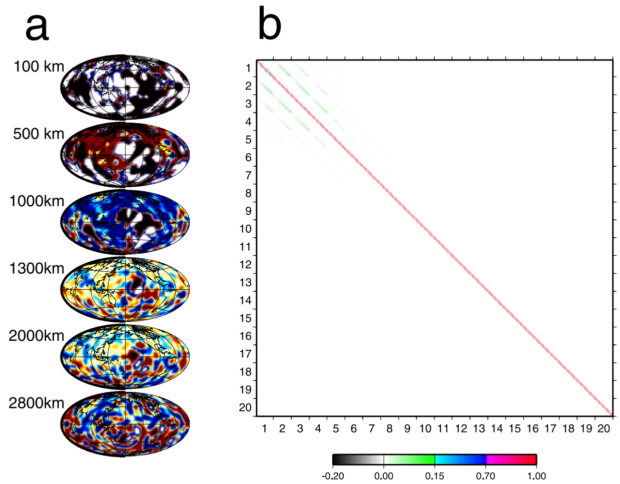

Figure 1. (a) Underdamped *P*-velocity model at six chosen depths in the Earth's mantle, and (b) R derived in the same inversion. Relative velocity heterogeneities range between 1% (dark blue) to −1% (dark red). For heterogeneities of amplitude >1%, the color scale saturates, and becomes white (for fast anomalies) or black (slow) over 3%. Each row/column of R corresponds to a "radial spline × horizontal spline" couple; within each row/column entries are grouped by radial splines; the radial splines are indexed from shallowest (1) to deepest (20). I have averaged R so that each pixel here represents 20 × 20 of its actual entries: this way, coefficients of close horizontal splines are merged in the same pixel; only trade-off between radial splines remains visible, in the form of nonzero bands parallel to the diagonal.

3. Application to ISC *P*-Wave Travel Time Data

[9] I employ the data set of *Antolik et al.* [2003], including $m \sim 626{,}000$ "summary" travel time observations, derived, after further relocation of all seismic sources, from the recompilation by *Engdahl et al.* [1998] of International Seismological Centre (ISC) data. No weighting is applied to the summary data. I choose to express the solution as a linear combination of the products of 362 horizontal equally spaced spherical splines [*Wang and Dahlen*, 1995], and 20 equal, and equally spaced, radial cubic B splines (the number of free parameters is therefore $n = 7240$); splines are more efficient than blocks in representing a complicate function with a limited number of free parameters [*Lancaster and Šalkauskas*, 1986; *Boschi*, 2001].

[10] I implement equations (3) and (5) via Cholesky factorization of the symmetric, positive-definite matrix $\mathsf{A}^T \cdot \mathsf{A} + \mathsf{D}$, the most efficient non-iterative algorithm for solving linear least-squares problems [e.g., *Trefethen and Bau*, 1997, p. 172; *Press et al.*, 1992, section 2.9], employed in global tomography by, for example, *Su et al.* [1994], and *Antolik et al.* [2003].

[11] As opposed to what stated, for example, by *Zhao* [2001], once the generalized inverse is found the implementation of (5) is not much more time consuming than that of (3); also, since $m \gg n$, the $n \times n$ matrix $\mathsf{A}^T \cdot \mathsf{A}$, although often denser than A, does not necessarily require a larger memory storage.

[12] The most time-consuming step of the process is the computation of $\mathsf{A}^T \cdot \mathsf{A}$, which I perform directly, adding up the contribution of each datum: finding $\mathsf{A}^T \cdot \mathsf{A}$ from A would take longer. On the fastest multiprocessor shared-memory servers available to me (by far not the fastest available on the market), computation of $\mathsf{A}^T \cdot \mathsf{A}$ takes about twenty-four hours, if I parallelize it by dividing the data set into several subsets, find $\mathsf{A}^T \cdot \mathsf{A}$ for each subset, and sum the results. After computing $\mathsf{A}^T \cdot \mathsf{A}$, which has to be done only once, x_{LS} and R can be derived in a time ranging between a few hours and a few minutes, depending on the machine and using about eight processors (single-processor LSQR typically takes hours longer). Library routines provided with the computers in question allowed me to make use of parallel Cholesky algorithms with a minimum programming effort (some basic MPI).

3.1. Data Coverage, Noise and Regularization

[13] It is well known that regularization ("damping") is essential to the solution of global tomographic inverse problems [e.g., *Boschi and Dziewonski*, 1999]. Parallel Cholesky factorization is a quite fast procedure (much faster than sequential LSQR), and numerous differently regularized inversions can be carried out in reasonable time, before choosing the optimal regularization scheme.

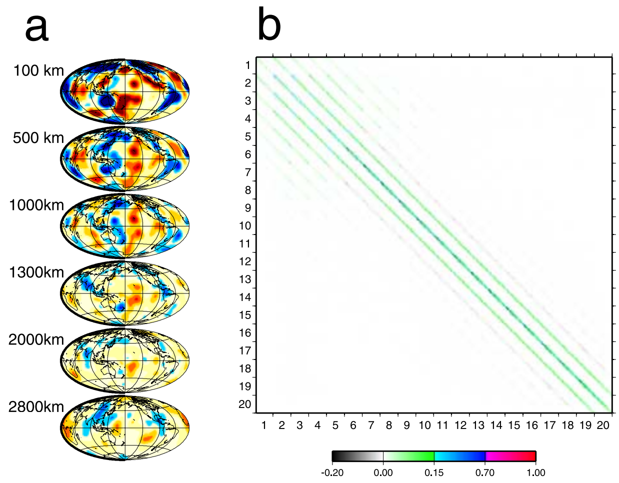

Figure 2. Same as Figure 1, but a more adequate damping scheme has been applied in the inversion.

For simplicity, and because my parameterization is inherently smooth with respect to the wavelength of the heterogeneities that I expect to map, I make here the simple choice that D be equal to a factor λ times the $n \times n$ identity matrix; for a spline parameterization, this is approximately equivalent to size-damping [*Boschi*, 2001]. Naturally, the algorithm works independently of the damping scheme.

[14] I show in Figure 1 a tomographic image (a), and corresponding R (b), derived with a very weak damping: I chose λ to be $\sim 10^6$ times smaller than the mean value of the diagonal entries of $\mathsf{A}^T \cdot \mathsf{A}$ (lower values of λ resulted in $\mathsf{A}^T \cdot \mathsf{A}$ being "too singular" for Cholesky factorization to be feasible). R is too large to be plotted entirely on one figure: for each 20×20 block of R I sum all entries and divide the result by 20. R is very close to I, indicating that the quality of data coverage would grant, in the absence of noise in the measurements, an almost perfect resolution. On the other hand, the undamped solution in Figure 1a is characterized by too strong gradients and too large amplitudes to be physically acceptable: more severe regularization is needed to counter the effect of noise.

[15] Figure 2 shows model (a) and R (b) derived with a value of λ of the same order of magnitude as the mean value of the diagonal entries of $\mathsf{A}^\mathsf{T} \cdot \mathsf{A}$. The image of Figure 2a correlates well with the *P*-velocity models discussed by *Becker and Boschi* [2002]. Nevertheless, the averaged plot of R in Figure 2b shows that nonnegligible trade-offs, accompanied by a significant loss of amplitude (diagonal entries of R are < 1), exist in the solution model. As to be expected, resolution is particularly poor in the upper mantle, where teleseismic ray paths are almost vertical and data coverage is then limited to areas of dense sismicity, or to the proximity of seismic stations.

[16] The tenth diagonal block of R from Figure 2b, associated to the radial spline centered at $\sim$1450 km depth, is shown in Figure 3. Nonzero off-diagonal entries now identify trade-offs between coefficients of horizontal splines at that depth. As only a small portion of R is shown, smoothing becomes unnecessary, and each pixel of the image corresponds to one entry of the matrix.

[17] Figure 3 shows that horizontal resolution at this depth is good, but not perfect. Off-diagonal nonzero fringes indicate that coefficients of neighboring splines are coupled. Particularly in the southern hemisphere (larger indices), covered by fewer data [*Boschi*, 2001], a certain loss of amplitude is visible. An analogous plot (not shown here) of R as derived in the undamped inversion (Figure 1), shows at this depth almost perfect horizontal resolution.

4. Conclusions

[18] The direct implementation of the "exact" (non-iterative) least-squares formulae (3) and (5), via parallel Cholesky factorization of $\mathsf{A}^T \cdot \mathsf{A} + \mathsf{D}$, makes it possible to determine rapidly the least squares solution, and resolution matrix R of very large inverse problems. With similar approaches, it should now be possible to evaluate efficiently other measures of resolution and covariance [*Menke*, 1989, chapter 4].

[19] The images derived here are of intermediate nominal resolution, equivalent to those of *Antolik et al.* [2003], with $n \sim 10{,}000$ model coefficients; modern multiprocessor shared-memory computers allow applications to problems of much higher nominal resolution, the main limiting factor being their RAM, which should be $\geq n^2 \times 4$ bytes.

[20] The resolution matrix is the best possible measure of model resolution. Naturally, R depends strongly on regularization, and estimates of model resolution should take

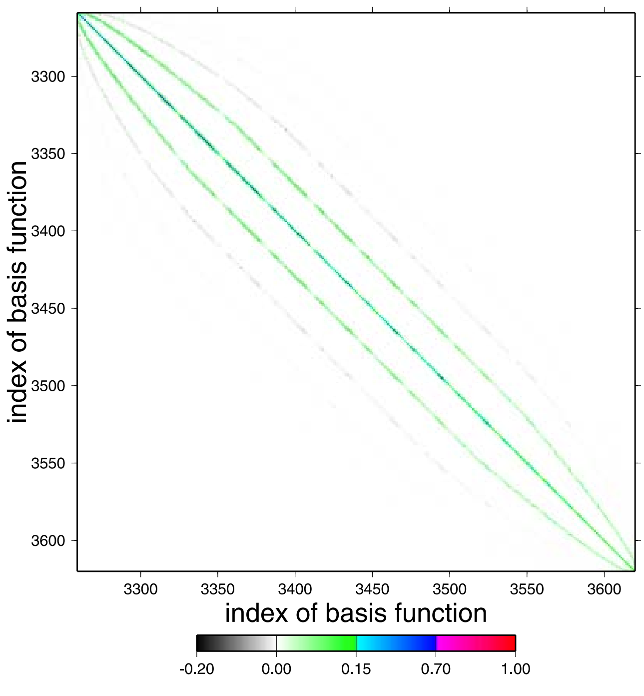

Figure 3. Tenth diagonal block of R, without averaging, showing trade-off between coefficients of horizontal splines associated with the tenth radial spline (depth $\sim$1450 km). Horizontally, the basis function index increases West to East (fast direction), and North to South. Most tradeoff occurs with immediate East and West (nonzero entries adjacent to the diagonal) and North and South (nonzero bands away from the diagonal) neighbors. As the spline grid is equally spaced, the number of its nodes decreases with increasing (positive or negative) latitudinal range, hence the convergence of off-diagonal bands.

account of the regularization scheme that had to be applied in the inversion. With a very weak damping, barely sufficient for $\mathsf{A}^T \cdot \mathsf{A}$ not to be singular, I have found R to be very close to identity, but the least squares solution thus obtained is not physically acceptable. A more strongly regularized inversion leads to a more reliable model (Figure 2), and the differences in R as found in the two cases evidence the specific effects of limits in data quality, as opposed to limits in data coverage.

[21] Tomographers attempting to derive high resolution images of the Earth should be aware of the severe limits imposed by the quality of available data. As resolution is not everywhere constant, but higher in regions of more uniform coverage, ad-hoc parameterization and regularization schemes can be designed to stabilize the solution in undersampled areas, and avoid overdamping it in regions whose short-wavelength structure can be properly constrained.

[22] **Acknowledgments.** Thanks to M. Antolik, A. Cherchi, A. Dziewonski, G. Ekström, P. Gasparini, Y. J. Gu, S. Judenherc, K. Larson, D. Melini, A. Navarra, A. Piersanti, G. Soldati, D. Vasco, A. Zollo. I made use of computers at Harvard University and INGV-Roma. All figures were produced with Generic Mapping Tools (GMT) [*Wessel and Smith*, 1991]. My research is funded by Ministero dell'Istruzione, Università e Ricerca.

References

Antolik, M., Y. J. Gu, G. Ekström, and A. M. Dziewonski, J362D28: A new joint model of compressional and shear velocity in the Earth's mantle, *Geophys. J. Int.*, *153*, 443–466, 2003.

Becker, T. W., and L. Boschi, A comparison of tomographic and geodynamic mantle models, *Geochem. Geophys. Geosyst.*, *3*, doi:10.1029/2001GC000168, 2002.

Boschi, L., *Applications of linear inverse theory in modern global seismology*, thesis, Harvard Univ., Cambridge, 2001.

Boschi, L., and A. M. Dziewonski, "High" and "low" resolution images of the Earth's mantle: Implications of different approaches to tomographic modeling, *J. Geophys. Res.*, *104*, 25,567–25,594, 1999.

Engdahl, E. R., R. D. van der Hilst, and R. P. Buland, Global teleseismic earthquake relocation with improved travel times and procedures for depth determination, *Bull. Seism. Soc. Am.*, *88*, 722–743, 1998.

Lancaster, P., and K. Šalkauskas, Curve and surface fitting—An introduction, Academic, San Diego, 1986.

Leveque, J. J., L. Rivera, and G. Wittlinger, On the use of the checker-board test to assess the resolution of tomographic inversions, *Geophys. J. Int.*, *115*, 313–318, 1993.

Menke, W., *Geophysical Data Analysis: Discrete Inverse Theory*, rev. ed., Academic, San Diego, 1989.

Minkoff, S. E., A computationally feasible approximate resolution matrix for seismic inverse problems, *Geophys. J. Int.*, *126*, 345–359, 1996.

Nolet, G., R. Montelli, and J. Virieux, Explicit, approximate expressions for the resolution and a posteriori covariance of massive tomographic systems, *Geophys. J. Int.*, *138*, 36–44, 1999.

Nolet, G., R. Montelli, and J. Virieux, Reply to comment by Z. S. Yao, R. G. Roberts and A. Tryggvason on 'Explicit, approximate expressions for the resolution and a posteriori covariance of massive tomographic systems', *Geophys. J. Int.*, *145*, 315, 2001.

Paige, C., and M. Saunders, LSQR: An algorithm for sparse linear equations and sparse least squares, *ACM Trans. Math. Software*, *8*, 43–71, 1982.

Press, W. H., S. A. Teukolsky, W. T. Vetterling, and B. P. Flannery, *Numerical Recipes in Fortran, Second Edition*, Cambridge Univ. Press, Cambridge, 1992.

Spetzler, J., J. Trampert, and R. Snieder, The effect of scattering in surface wave tomography, *Geophys. J. Int.*, *149*, 755–767, 2002.

Su, W.-J., R. L. Woodward, and A. M. Dziewonski, Degree 12 model of shear velocity heterogeneity in the mantle, *J. Geophys. Res.*, *99*, 6945–6981, 1994.

Trefethen, L. N., and D. Bau, *Numerical Linear Algebra*, SIAM, Philadelphia, PA, 1997.

Vasco, D. W., R. J. Pulliam, and L. R. Johnson, Formal inversion of ISC arrival times for mantle P-velocity structure, *Geophys. J. Int.*, *113*, 586–606, 1993.

Vasco, D. W., L. R. Johnson, and O. Marques, Global Earth structure: Inference and assessment, *Geophys. J. Int.*, *137*, 381–407, 1999.

Vasco, D. W., L. R. Johnson, and O. Marques, Resolution, uncertainty, and whole-Earth tomography, *J. Geophys. Res.*, *108*(B1), 2022, doi:10.1029/2001JB000412, 2003.

Wang, Z., and F. A. Dahlen, Spherical-spline parameterization of three-dimensional Earth models, *Geophys. Res. Lett.*, *22*, 3099–3102, 1995.

Wessel, P., and W. H. F. Smith, Free software helps map and display data, *Eos, Eos Trans. AGU*, *72*, 445–446, 1991.

Yao, Z. S., R. G. Roberts, and A. Tryggvason, Calculating resolution and covariance matrices for seismic tomography with the LSQR method, *Geophys. J. Int.*, *138*, 886–894, 1999.

Yao, Z. S., R. G. Roberts, and A. Tryggvason, Comment on 'Explicit, approximate expressions for the resolution and *a posteriori* covariance of massive tomographic systems' by G. Nolet, R. Montelli, and J. Virieux, *Geophys. J. Int.*, *145*, 307–314, 2001.

Zhao, D., New advances of seismic tomography and its applications to subduction zones and earthquake fault zones: A review, *The Island Arc*, *10*, 68–84, 2001.

Zhang, J., and G. A. McMehan, Estimation of resolution and covariance for large matrix inversions, *Geophys. J. Int.*, *121*, 409–426, 1995.

Zollo, A., L. D'Auria, R. De Matteis, A. Herrero, J. Virieux, and P. Gasparini, Bayesian estimation of 2-D *P*-velocity models from active seismic arrival time data: Imaging of the shallow structure of Mt. Vesuvius (Southern Italy), *Geophys. J. Int.*, *151*, 566–582, 2002.

L. Boschi, Università di Napoli Federico II, Dipartimento di Fisica, Via Cinthia, 80126, Naples, Italy. (lapo.boschi@na.infn.it)